

Investigations of the Diffuse Ultrasonic Field in Low-Frequency Sonophoresis and Liposomes on Skin Permeability

Yi-Cheng Huang^{1*}, Shih-Kuang Yang²

¹Department of Mechanical Engineering, Cheng Shiu University, Taiwan 833, RO China

²Department of Mechanical and Electro-Mechanical Engineering, National Sun Yat-Sen University, Taiwan 804, RO China. E-mail : huang@csu.edu.tw

Abstract: This study investigated the permeability of skin to the transdermal delivery of liposomes with or without the application of a diffuse low frequency ultrasonic field. Specimens were exposed to ultrasound at frequencies of 20 and 60 kHz and intensities of 0.19 and 0.43 W/cm². In these experiments, the diffuse ultrasonic field was produced using an inclined incident transducer and specially designed wedge. The samples exposed to ultrasound were compared to unexposed samples by recording the permeated depth of rhodamine into the skin. An ultrasonic frequency of 60 kHz at an intensity of 0.43 W/cm² enhanced the permeated depth to a higher degree than other tested parameter combinations. In general, ultrasound of higher applied intensity resulted in greater depth of permeation than lower intensity.

[Yi-Cheng Huang, Shih-Kuang Yang. **Investigations of the Diffuse Ultrasonic Field in Low-Frequency Sonophoresis and Liposomes on Skin Permeability.** *Life Sci J* 2013;10(2):271-275] (ISSN:1097-8135). <http://www.lifesciencesite.com>. 43

Keywords: low frequency ultrasound, liposome, diffuse field, designed wedge

1. Introduction

The ultrasound technology has been shown to be more convenient tools in medicine and biology [1-3]. Under suitable conditions, ultrasound has been shown to enhance transdermal transport through a phenomenon referred to as sonophoresis [4]. Ultrasound at low frequencies has demonstrated greater effectiveness than at high frequencies [5-6], due to the promotion of cavitation, which is important to skin permeabilization [7]. Acoustic cavitation can be classified as either stable cavitation which corresponds to steady oscillations of bubbles or transient cavitation which corresponds to a rapid growth followed by a rapid collapse. Many methods of enhancing cavitation have been reported, such as the use microspheres, silica particles, and ultrasonic contrast agents to enhance cavitation [8].

The composite structure of liposome is made of phospholipids often containing trace amounts of other molecules. The size of the liposomes varies from the low micrometer range to tens of micrometers. Liposomes are artificially prepared vesicles made of a lipid bilayer, which are filled with drug for delivery to treat cancer and other diseases. Dahlan et al. investigated the influence of low frequency ultrasound and liposomes on skin [8]. It was observed that liposomes are capable of repairing damage of to the skin, which limits drug permeation. The influence of liposomes is often evident within 5 min of application, and smaller liposomes have proven more effective at repairing skin disruptions resulting from sonication. It is believed that the repair of skin by liposomes depends on the extent of the disruption

caused by ultrasound.

Although ultrasound is capable of assisting in the transdermal delivery of drugs in liposomes, a number of questions remain. Exposing high intensity ultrasound increases the temperature of the liquid, which damages the liposome and renders the drug ineffective. Thus, this study discusses liposomes in solution (with and without the influence of an ultrasonic field), and compares the permeation depth of material entrapped within liposomes (rhodamine B). A diffuse ultrasonic field was produced using a combination of an inclined incident transducer and a specially designed wedge. To prevent the appearance of thermal effects, the transducer was driven with lower ultrasonic intensity. Two driving frequencies were selected to examine the distribution conditions and the depth of skin permeation.

2. Materials and methods

2.1 Diffuse Ultrasonic and Measurement Field

We adopted the diffuse field theory of Sabine to create a uniform sound field for the radiation experiment [10]. According to this theory, the ultrasonic beam must be obliquely incident to the finite boundary, such repeated reflection of the sound waves produces a uniform sound field within the space. The cuboid acrylic wedge, with a bottom area of 62×65 mm and the height of 120 mm was shown schematically in Fig. 1 [11]. The top corner of the exposed wedge provided an oblique, triangle plane of length of 75 mm to mount the ultrasonic transducer. The ultrasonic beam of the transducer was incident from one edge toward the boundary of the wedge at the far end. The exposure area (indicated in the figure)

was used to contact the skin samples. The sampling positions of the exposure area are the same as our previous study and shown in the color mapping of the permeated depth distribution of result figures (Fig. 3). The depth of permeation was measured in six randomly selected points of each sampling position using a Nikon C1 plus confocal microscopy. A sampling position of each of six randomly selected regions of each specimen was taken. The mean values of permeated depth in the six regions indicates the distribution of depth at a sampling position. The ultrasonic transducer was positioned above sampling position A1 of the exposure area. Two custom built transducers with operating frequencies of 20 and 60 kHz (BroadSound Corporation, Taiwan, R. O. C.) were used for the application of ultrasound. The exposure and measurement system for the diffusion field comprised a specially developed ultrasonic transducer capable of producing a diffuse sound field, as shown in Fig. 2. The transducer was driven by a continuous sine wave from a function generator (GW Instek SFG-830). The intensity of the sound field was measured using a miniature PVDF ultrasonic hydrophone probe (Force Institute MH28-10). In this experiment, the output intensities were set at 0.19 and 0.45 W/cm². The signal obtained from the hydrophone was analyzed using a digitizing oscilloscope (LeCroy WaveSurfer 422). Exposure of skin samples to ultrasound was limited to 5 minutes to prevent increasing the skin temperature. All experiments were performed at room temperature. When the skin samples were exposed or sham-exposed to ultrasonic irradiation, the permeated depth distribution of liposomes, with and without the influence of ultrasonic waves, was observed.

2.2 Material and skin preparation

Skin exposure experiments were carried out in vitro with full thickness skin of the ear of Yorkshire pigs. Superfluous tissues such as fat and muscle was removed. The skin was cut into squares (10×10 cm), and stored in a freezer until used. Egg yolk phosphatidylcholine (EPC) and cholesterol (Sigma Chemical Co., St. Louis, MO) in a molar ratio of 4:1 were mixed in a round-bottomed flask. A fluorescence materials (rhodamine) was dissolved in the suspension prepared by dissolving in chloroform. The organic solvent was subsequently evaporated under vacuum using a stream of nitrogen to remove traces of chloroform. The resulting dried lipid film was dispersed with a buffer solution (Hepes: 0.1 M, pH 5). The solution was vortex mixed above the room temperature to yield lipid suspensions. Lipid suspensions then underwent mechanical shaking for 30min after which an ultrasonic processor was used to crush the lipid membranes and obtain liposomes with a diameter of 200 nm.

3. Results and discussions

Table 1 presents the permeated depth of liposomes at each sampling position for exposure or sham-exposure to ultrasonic irradiation of 2 different intensities. In this table, the permeated depth of liposome is presented in micrometers. Sham irradiation experiments were used to compare the influence of the ultrasonic irradiation on the liposomes and to measure the permeated depth after maintaining the liposome solution on the skin for approximately 30 min. Fig. 3 shows the permeated depth distribution of the exposure area of the skin samples exposure to ultrasound, based on a color plot. Sampling positions A1 to A9 indicate the relative position in the exposure area. The color scale is provided by MATLAB package, and expanded from 130 to 200 μm in the Z-axis.

Figures 3(a)-(d) plot the distribution of permeated depth with ultrasound exposure obtained from the data in Table 1. In the experiment, the sound beam was incident into the cuboid acrylic wedge and produced a diffuse ultrasonic field. Figures 3(a)-(b) plot the results of exposure to an ultrasonic frequency of 20 kHz at an intensity of 0.19 or 0.45 W/cm², in which the distribution of permeated depth for the two intensities is from 148.3 to 181.7 μm. The average permeated depth of liposomes is 158 μm at low intensity and 159 μm at high intensity, as shown in Table 1. Researchers avoided thermal effects induced by ultrasound by preventing the transducer from coming into direct contact with the skin sample and reducing exposure time. Thus, the average values of permeated depth for the two exposed intensities are very close despite a more than twofold difference in exposure intensity. By comparison, the average permeated depth of the sham irradiation results increased to approximately 20 μm. Under an intensity of 0.19 W/cm², the greatest permeated depth is 181.7 μm in sampling position A6; with an intensity of 0.45 W/cm², the greatest depth is 173.3 μm in sampling position A5. The maximum permeated depth resulting from an exposure intensity of 0.19 W/cm² exceeded the results at 0.45 W/cm², however; the average value at 0.19 W/cm² is still lower than the average at 0.45 W/cm². In addition, with an intensity of 0.19 W/cm², the difference in permeated depth between maximum and minimum there is 31.7 μm, however; the difference value at 0.45 W/cm² is 25 μm. Clearly, lower exposure intensity creates greater difference on permeated depth. A comparison of the two different intensities at 20 kHz also shows that the higher intensity increases the average permeated depth, resulting in greater consistency in depth among the sampling positions.

Figures 3(c)-(d) plot the results of exposure to an ultrasonic frequency of 60 kHz at intensities of

0.19 and 0.45 W/cm². In these two images, the distribution of permeated depth for the two intensities is in the range of 148.3 - 190 μm. The average permeated depth is 167 at low intensity and 168 μm at high intensity, as shown in Table 1. Notably, the average results from the two exposure intensities of 0.19 or 0.45 at a frequency of 60 kHz clearly are similar to the results from exposure at 20 kHz with difference of just 1 μm. At 60 kHz, the average permeated depth at an exposure intensity of 0.45 W/cm² exceeds the sham-exposed result by 30 μm. The average permeated depth also exceeds the result at 20 kHz by 10 μm. As can be seen in the Table 1, at an intensity of 0.19 W/cm², the maximum permeated depth is 190 μm in sampling position A4. At an exposure intensity of 0.45 W/cm², the maximum depth is 185 μm in sampling position A2. The maximum permeated depth at an exposure intensity of 0.19 W/cm² exceeds that at 0.45 W/cm² about 5 μm. The average permeated depth at 0.19 W/cm² is still lower than that at 0.45 W/cm². In addition, with an intensity of 0.19 W/cm², the difference in permeated depth between maximum and minimum there is 41.7 μm, however; the difference value at 0.45 W/cm² is 33.3 μm. Thus, the same results occur for the two irradiation frequencies, in which the higher intensity increases the average permeated depth and provides greater consistency in depth among the various sampling positions on the skin sample.

Figure 4(a)-(d) show the influence of ultrasound exposure to more clearly elucidate the change in permeated depth between samples exposed or sham-exposed to ultrasonic irradiation. These figures plot the average values of permeated depth as a function of sampling position for various exposure intensity at frequencies of 20 and 60 kHz, respectively. Notably, the plotted data represent the arithmetic mean over the six sampling points at one sampling position. As seen in these figures, the permeated depth of

treated samples exceeds that of sham-exposed skin. In sampling position A1, the permeated depth of the exposed samples exceeds that of the control samples by more than 170 μm, except at a frequency of 20 kHz and intensity of 0.19 W/cm². Based on the dimensions of the wedge presented in Figure 2, the sound beam has an incident angle of 45°. With the application of ultrasound, the sound wave is initially reflected from the boundary of the wedge, such that the reflected beam points to the sampling positions A1, A2, A4 and A5. A portion of the reflected sound wave penetrates through the wedge to produce greater acoustic radiation force. The acoustic radiation force influences the liposomes and pushes them down through the skin. In these four figures, the smallest difference in permeated depth between the exposed and sham-exposed samples appeared in sampling position A7. It is possible that the ultrasonic energy passing through the wedge in position A7 was lower than the other positions. The sound waves are reflected a lot of times before penetrated through the wedge, and this may reduce energy and decrease the permeated depth.

4. Conclusions

This study examined a number of issues. First, a wedge was designed with an inclined incident angle to investigate the permeated effects of the diffuse ultrasonic field. Second, ultrasonic frequencies of 20 and 60 kHz were applied at intensities of 0.19 and 0.45 W/cm². Third, the average permeated depth of liposomes in each experiment were observed and the permeated depth distribution were compared at the sampling position on the skin sample. An ultrasonic intensity of 0.45 W/cm² and a frequency of 60 kHz caused the liposomes to permeate the skin more effectively than other setup. The wedge designed at an inclined incident angle with an appropriate ultrasonic intensity and frequency could induce liposomes to permeate skin samples more deeply.

Table 1. Permeated depth in various sampling positions are exposed to ultrasound of 20 and 60 kHz frequencies at two output intensities. The recorded values are in micrometers. In this table, the (AVG) is the average permeated depth in the series of sampling positions.

| Sampling position \ Frequency | Sham exposed | 20 kHz | | 60 kHz | |
|-------------------------------|--------------|------------------------|------------------------|------------------------|------------------------|
| | | 0.19 W/cm ² | 0.45 W/cm ² | 0.19 W/cm ² | 0.45 W/cm ² |
| A1 | 130 | 150 | 171.7 | 170 | 173.3 |
| A2 | 130 | 165 | 158.3 | 168.3 | 185 |
| A3 | 133.3 | 155 | 150 | 175 | 165 |
| A4 | 136.7 | 166.7 | 161.7 | 190 | 165 |
| A5 | 145 | 171.7 | 173.3 | 160 | 176.7 |
| A6 | 141.7 | 181.7 | 158.3 | 163.3 | 168.3 |
| A7 | 145 | 156.7 | 153.3 | 148.3 | 158.3 |
| A8 | 145 | 163.3 | 153.3 | 155 | 171.7 |
| A9 | 138.3 | 173.3 | 148.3 | 173.3 | 151.7 |
| AVG | 138 | 158 | 159 | 167 | 168 |

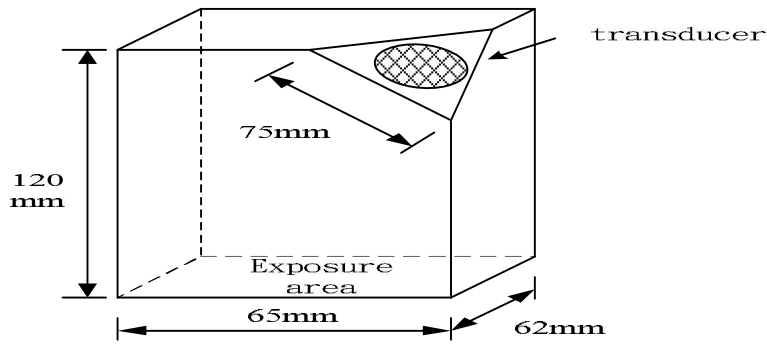


Figure 1. Dimensions of the exposure wedge. The orientation of the transducer is fixed in the corner of the chamber [11].

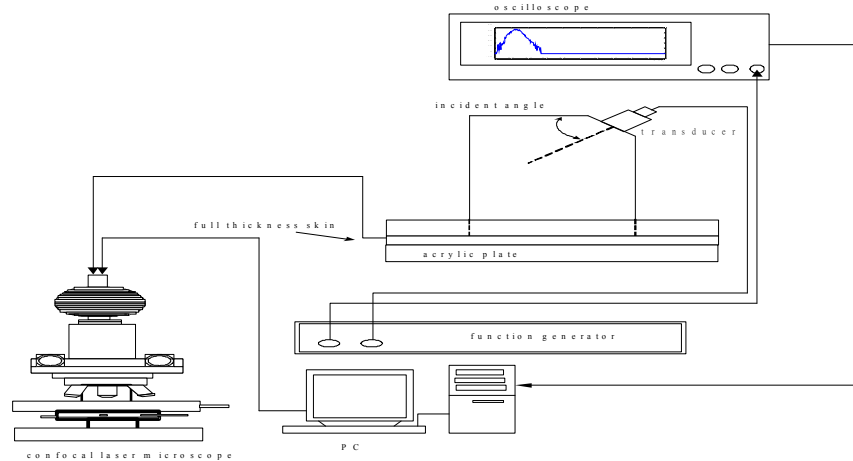


Figure 2. Schematic diagram of the isonation and measurement apparatus used in the exposure experiments [11].

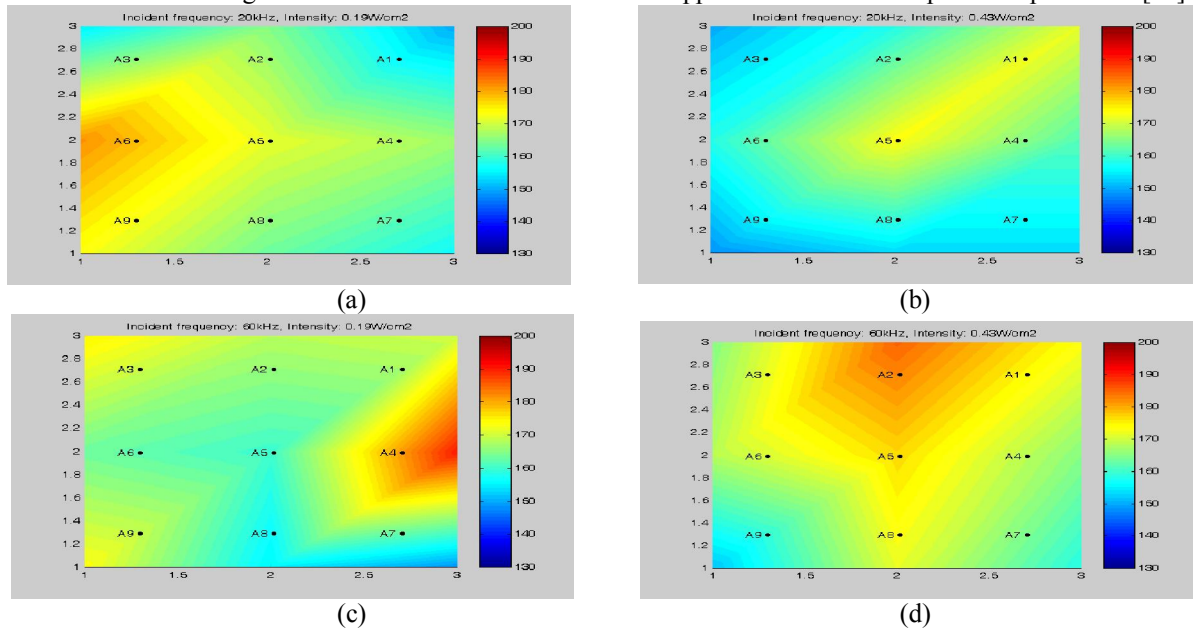


Figure 3. Color mapping of the permeated depth distribution for the skin sample at exposure frequencies of 20 and 60 kHz. Results were obtained from different intensities: (a)(b) results for intensities of 0.19 and 0.45 W/cm^2 at 20 kHz; (c)(d) results for intensities of 0.19 and 0.45 W/cm^2 at 60 kHz.

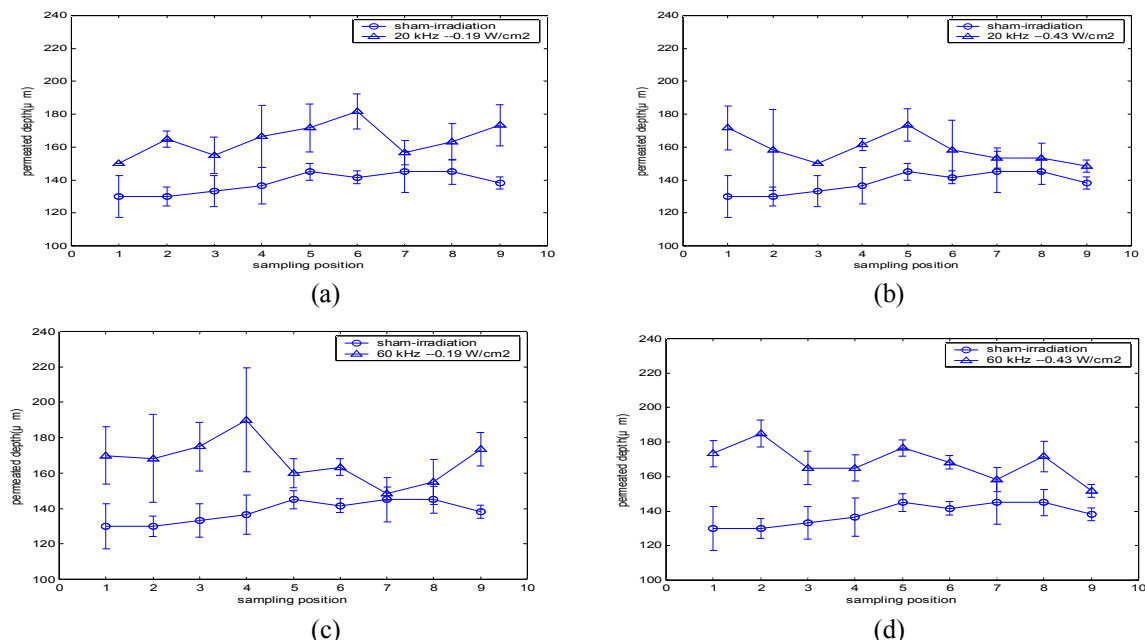


Figure 4. Average values of permeated depth as a function of sampling position for the skin sample at exposure frequencies of 20 and 60 kHz. The results were obtained for different intensities: (a)(b) results for intensities of 0.19 and 0.45 W/cm² at 20 kHz, (c)(d) results for intensities of 0.19 and 0.45 W/cm² at 60 kHz.

Corresponding Author:

Yi-Cheng Huang, PhD.

E-mail : huang@csu.edu.tw.

References

1. Aysha I.Z. Badawi, Randa F Abd Al Salam, Amal A El Wahab. Endothelial dysfunction in systemic lupus erythematosus. *Life Sci J*, 2010;7(4):98-104
2. Aboserea M, Abdelgawad M, Wafik W. Early detection of breast cancer among females at fakous district, sharqia governorate, egypt. *Life Sci J*, 2011,8(1):196-203
3. Amal Ahmed, Sahar Maklad, Ghada Hussein, Ingy Badawy, Alaa Abou Zeid and Said El-Feky. Assessment of the role of interleukin-18 in diagnosis of hepatocellular carcinoma related to hepatitis C virus infection. *Life Sci J*, 2011,8(4):1154-1158
4. Hideo Ueda, Mizue Mutoh, Toshinobu Seki, Daisuke Kobayashi and Yasunori Morimoto. Acoustic cavitation as an enhancing mechanism of low-frequency sonophoresis for transdermal drug delivery. *Biol Pharm Bull*, 2009,32(5):916-920
5. Boucaud A, Garrigue MA, Machet L, Vaillant L and Patat F. Effect of sonication parameters on transdermal delivery of insulin to hairless rats. *J Control Rel*, 2002,81:113-119
6. Mitragotri S and Kost J. Low-frequency sonophoresis: a noninvasive method of drug delivery and diagnostics. *Biotechnol Prog*, 2000,16:488-492
7. Mitragotri S, Blankschtein D, Langer R. Transdermal Drug Delivery Using Low Frequency Sonophoresis. *Pharm Res*, 1996, 13:411-420
8. Madanshetty SI and Apfel RE. Acoustic micro cavitation: Enhancement and applications. *J Acoust Soc Am*, 1991;90,1508-1514
9. Dahllana A, Alpara HO, Murdan S. An investigation into the combination of low frequency ultrasound and liposomes on skin permeabilitys. *Int J of Pharm*, 2009, 379(1):139-142
10. Sabine WC. *Collected Papers on Acoustics*, Dover, New York, 1964
11. Huang YC and Yang SK. Effects of Designed Ultrasonic Field in Different Frequency Sonophoresis Using the Carrier of Liposomes. *Life Sci J*, 2012,9(2):154-159.

3/14/2013